bioRxiv preprint doi: https://doi.org/10.1101/2023.11.04.565631; this version posted November 5, 2023. The copyright holder for this preprint (which was not certified by peer review) is the author/funder, who has granted bioRxiv a license to display the preprint in perpetuity. It is made available under aCC-BY 4.0 International license.

An injectable in situ crosslinkable platform for ultra-long-acting delivery of hydrophilic therapeutics

Sohyung Lee[1,2,3]†, Spencer Zhao[2,3]†, Xinyang Chen[2,3], Lingyun Zhu[2,3], John Joseph[1,2,3], Eli Agus[2,3], Shumaim Barooj[2,3], Helna Baby Mary[2,3], Purna Shah[2,3], Kai Slaughter[2,3], Krisco Cheung[2,3], James N Luo[1,4], Jingjing Gao[1,2,3,5], Dongtak Lee[1,2,3], Jeffrey M Karp[1,2,3,6,7,8]* and Nitin Joshi[1,2,3]*

[1] Harvard Medical School, Boston, MA, USA

[2] Center for Accelerated Medical Innovation, Department of Anesthesiology, Perioperative and Pain Medicine, Brigham and Women's Hospital, Boston, MA 02115, USA

[3] Center for Nanomedicine, Department of Anesthesiology, Perioperative and Pain Medicine, Brigham and Women's Hospital, Boston, MA, USA

[4] Department of Surgery, Brigham and Women's Hospital, Boston, MA 02115, USA

[5] College of Engineering, University of Massachusetts Amherst, MA, USA

[6] Harvard–Massachusetts Institute of Technology Division of Health Sciences and Technology, Massachusetts Institute of Technology, Cambridge, MA 02139, USA

[7] Broad Institute, Cambridge, MA 02142, USA.

[8] Harvard Stem Cell Institute, Cambridge, MA 02138, USA

†Equal contribution

*Corresponding authors: J.M.K. (jmkarp@bwh.harvard.edu) and N.J. (njoshi@bwh.harvard.edu)

Abstract

Although hydrophilic drugs represent a large proportion of all therapeutics used to treat and manage chronic diseases, achieving their ultra-long-term delivery via an injectable system remains a major challenge. Implants have demonstrated potential for long-term delivery of both hydrophobic and hydrophilic drugs; however, they require invasive insertion process in a sterile setting, which restricts their suitability for resource-limited settings.

bioRxiv preprint doi: https://doi.org/10.1101/2023.11.04.565631; this version posted November 5, 2023. The copyright holder for this preprint (which was not certified by peer review) is the author/funder, who has granted bioRxiv a license to display the preprint in perpetuity. It is made available under aCC-BY 4.0 International license.

Furthermore, implants tend to be more susceptible to local inflammation when compared to injectable alternatives. Here we report a solvent free, injectable, biodegradable, and in situ crosslinking depot (ISCD) platform for ultra-long term release of hydrophilic drugs. ISCD consists of a low molecular weight liquid pre-polymer methacrylated polycaprolactone (PCL). Both hydrophilic and hydrophobic drugs can be suspended/dissolved in the liquid polymer, and when injected along with a radical initiator and an accelerator, the polymer crosslinks *in situ*, resulting in a solid monolithic and degradable depot, integrating the unique advantages of injectability and retrievability. Low molecular weight PCL forms a dense mesh, which limits water influx/efflux and hence reduces the drug release. Liquid state of the polymer obviates the need for solvent, minimizing initial burst release due to the solvent exchange process, as observed with *in situ* forming implants. Drug release and ISCD degradation can be tailored by modifying their polymer network via altering the concentration of accelerator and initiator, molecular weight of methacrylated PCL, or by incorporation of a hydrophilic polymer or a non-crosslinking polymer. We demonstrated sustained release of seven hydrophilic drugs with varying solubility or drug combinations for over seven months *in vitro*. Ultra-long term drug release and depot degradation was also demonstrated in rats for at least six months without any evidence of local inflammation or fibrosis. Excitingly, the platform also enabled ultra-long term release of a model hydrophobic drug – tacrolimus for at least six months. To the best of our knowledge, this marks the first successful demonstration of an ultra-long term delivery of hydrophilic drugs using an injectable formulation. This platform holds promise for developing ultra-long acting therapies across a wide range of diseases.

Introduction

Patient adherence to medications is a major obstacle towards achieving effective treatment of numerous diseases, especially in the treatment of chronic conditions where patients are required to take therapeutics throughout their entire life[1-3]. Sustained release technologies, such as long-acting injectables and implants simplify dosing schedules and minimize side effects by maintaining steady blood levels of the drug[4-11]. These benefits reduce the need for frequent medical visits and enhance treatment regimen adherence, which is particularly advantageous in developing countries with limited healthcare infrastructure and resources.

Multiple long-acting implants and injectables are in clinical use for the treatment and prevention of different diseases.[12, 13] Although implantable devices have shown success for the long-term delivery of both hydrophobic[9,

bioRxiv preprint doi: https://doi.org/10.1101/2023.11.04.565631; this version posted November 5, 2023. The copyright holder for this preprint (which was not certified by peer review) is the author/funder, who has granted bioRxiv a license to display the preprint in perpetuity. It is made available under aCC-BY 4.0 International license.

[14-18] and hydrophilic drugs[9, 16], they require invasive, time-consuming medical procedures for insertion, which may pose significant challenges, particularly in low resource settings and low-middle income countries. Furthermore, implants in general tend to be more susceptible to local inflammation when compared to injectable alternatives.[19, 20] Conventional injectable platforms such as microparticles, and *in situ*-forming implants (ISFI) have been documented to achieve prolonged release of hydrophobic drugs but have poor ability to achieve similar long-term release of hydrophilic drugs[21-24]. In the case of ISFI, which typically consist of a hydrophobic polymer, poly(lactic-co-glycolic acid) (PLGA) dissolved in N-methyl-2-pyrrolidone (NMP), efflux of the solvent during phase conversion tends to release a significant amount of drug as initial burst, which increases with the hydrophilicity of the drug. Microparticles and ISFI based approaches also promote significant influx and efflux of water due to their large pores, leading to fast diffusion of hydrophilic drugs.[14, 23, 25] Moreover, certain long-acting injectable approaches employ manufacturing processes such as wet-milling,[26, 27] which require the drug to be hydropbohic and are fundamentally incompatible with hydrophilic drugs. [6, 8, 12, 14, 22, 28]

Hydrophilic drugs constitute a major fraction of all the drugs used for the treatment and management of chornic conditions. Examples include antipsychotics (e.g., olanzapine, risperidone, and quetiapine), antidepressants (e.g., fluoxetine, sertraline, and citalopram), anticonvulsants (e.g., carbamazepine, phenytoin, and valproic acid), anti-inflammatory drugs (e.g., ibuprofen, naproxen, and celecoxib), antibiotics (e.g., amoxicillin, vancomycin, and gentamicin), and treatments for substance abuse (e.g., naltrexone, buprenorphine, and methadone), which often consist of hydrophilic drugs. Therefore, there is an unmet need to develop an injectable and biodegradable platform that enables ultra-long-term delivery of hydrophilic drugs. Additionally, the platform should be designed to allow for retrieval in the event of local or systemic drug toxicity.

Here, we report an extended-release injectable drug delivery platform, ISCD, capable of providing continuous delivery of both hydrophilic and hydrophobic drugs for 6 months, representing the first successful instance of prolonged delivery of hydrophilic drugs using an injectable system. The main component of ISCD is a vinyl end functionalized, low-molecular-weight liquid hydrophobic polymer – PCL. This polymer effectively suspends both hydrophilic and hydrophobic drugs, transitioning into a solid monolithic depot upon injection with a radical initiator and an accelerator. By using low molecular weight polymer, the polymer maintains liquid state, obviating need for the solvent, while achiving solid depot with dense mesh network upon polymerization. The ISCD's dense

bioRxiv preprint doi: https://doi.org/10.1101/2023.11.04.565631; this version posted November 5, 2023. The copyright holder for this preprint (which was not certified by peer review) is the author/funder, who has granted bioRxiv a license to display the preprint in perpetuity. It is made available under aCC-BY 4.0 International license.

mesh network and solvent-free nature attribute to the remarkably prolonged therapeutic release, effectively minimizing burst release. In vitro, ISCD demonstrated ultra-long-term release of multiple drugs of varying hydrophilicity for at least six months. Our data provide evidence that the ISCD platform offers multiple control handles to tune the release kinetics of the encapsulated drugs. These include concentration of cross-linking agents, molecular weight of the PCL, incorporation of a hydrophilic polymer or a non-cross-linking polymer. In vivo, ISCD formulations loaded with tenofovir alafenamide (TAF) or naltrexone (NAL) with water solubilities of 5.63 and 100 mg/mL, respectively, showed sustained release for at least six months with plasma concentrations within the therapeutic window. Impressively, ISCD also demonstrated ultra-long-term release of the hydrophobic drug tacrolimus (TAC), achieving sustained release for at least 200 days in vivo. We have thoroughly evaluated the biocompatibility, retrievability and drug delivery capabilities of our ISCD platform to ensure its safety and adaptability. ISCD has also demonstrated ultra-long-term release of various combinations of antiretroviral drugs used clinically to prevent and treat HIV. Overall, we believe that ISCD holds promise for further development as an ultra-long-acting platform for a variety of other diseases where patient adherence is critical.

Results

Synthesis and characteriazaion of ISCD

The main component of engineered injectable is low molecular methacrylated PCL which is biodegradable and biocompatible, and has been used previously in multiple FDA approved products. Drugs can be physically encapsulated in the polymer component by suspension or dissolution (Figure 1A). This mixture, prior to solidification, has a low enough viscosity to be injected with conventional 18-25 gauge needles and can also be molded into various shapes and potentially used as an implantable depot (Figure 1B). To prepare methcarylated PCL, PCL-diol and -triol were methacrylated via reaction with methacrylic anhydride (MAA) and triethylamine (TEA) to be polycaprolactone dimethylacrylate (PCLDMA) and polycaprolactone trimethylacrylate (PCLTMA) (Figure S1). When mixed with the radical initiator – benzoyl peroxide (BPO) and the accelerator – N,N-dimethyl-p-toluidine (DMT) which have been used clinically in the bone cements for past 50 years, radical polymerization of methcrylate PCL commences to create new carbon-carbon polymer chains, crosslinking the biodegradable polymer domains. Over time, hydrolysis of the original biodegradable polymer ester bonds allows gradual erosion of the depot, obviating the need for surgical removal (Figure S2). When mixed with 0.1, 0.3, and 0.5% BPO and

bioRxiv preprint doi: https://doi.org/10.1101/2023.11.04.565631; this version posted November 5, 2023. The copyright holder for this preprint (which was not certified by peer review) is the author/funder, who has granted bioRxiv a license to display the preprint in perpetuity. It is made available under aCC-BY 4.0 International license.

DMT, PCLDMA underwent a sol-gel transition to a monolithic depot within 9.3 ± 0.4, 5.0 ± 0.3, and 1.5 ± 0.3 minutes, respectively (Figure 1E), with a decrease in crosslinking time at higher polymerization agent concentrations. We demonstrated the sustained release of TAF, a hydrophilic drug with a water solubility of 5.63 mg/mL, over 200 days using either PCLDMA (Mn~630) or PCLTMA (Mn~1100), demonstrating the prolonged hydrophilic drug release capabilities of the methacrylated PCL-based long-acting injectables (Figure 1C). We encapsulated 30-150 mg/mL TAF in PCLDMA ISCDs and demonstrated that the release profiles from the ISCDs are similar over the range of drug loading (Figure 1D), demonstrating that the drug released is proportional to the drug loading (Figure S3A).

In situ implants, such as bone cement, often cause thermal tissue damage due to the high amount of heat generated during the polymerization process.[29] Therefore, we used differential scanning calorimetry (DSC) to quantify the exothermic heat released during the polymerization of PCLDMA with different concentrations of BPO/DMT and confirmed that there is no significant heat generation even at the higher BPO/DMT concentration. This alleviates concerns about potential thermal tissue damage during the procedure.

The implants should maintain their structural integrity even when subjected to significant external forces within the patient's body, a critical consideration given the intricate and dynamic mechanical conditions present in the human body. Therefore, the mechanical integrity is crucial for ensuring that the drug delivery system functions as intended throughout its lifecycle within the patient's body. To assess the mechanical properties of the PCLDMA ISCDs, we performed compression testing both with and without the presence of 90 mg/mL TAF to analyze their mechanical properties. The results showed that the modulus for ISCDs with and without TAF was 68.1 ± 10.3 and 67.2 ± 4.0 MPa, respectively, and the yield stress was 24.2 ± 1.1 and 25.9 ± 1.5 MPa, respectively (Figure 1G,H), indicating that the PCLDMA ISCDs exhibited a high level of structural rigidity. It is noteworthy that these mechanical properties align closely with those observed in clinically established solid implants[15, 30], which underscores the reliability and suitability of the ISCDs for drug delivery applications. Importantly, the inclusion of the drug does not compromise the structural integrity of the delivery system. This finding provides assurance that the drug remains adequately protected within the ISCDs and that these systems can efficiently deliver the drug without mechanical failure.

bioRxiv preprint doi: https://doi.org/10.1101/2023.11.04.565631; this version posted November 5, 2023. The copyright holder for this preprint (which was not certified by peer review) is the author/funder, who has granted bioRxiv a license to display the preprint in perpetuity. It is made available under aCC-BY 4.0 International license.

Another important property for the injectable implants is the rheological properties, because it can affect the ease of injection and ensure that the implant can be delivered effectively. We analyzed the viscosities of the ISCD prepolymer solutions and calculated the force required to inject the solutions (1 mL in 30 seconds with a 23 G nozzle) indirectly using the Hagen-Pouiselle equation[31]. The calculated injection forces for ISCD solutions with and without 90 mg/mL TAF are 64.0 ± 3.7 and 44.4 ± 7.8 N, respectively, showing an increase in viscosity and injection force with drug encapsulation. Both compositions exhibited values below 80 N, which is considered difficult for most people and therefore often considered the maximum acceptable injection force, demonstrating their superior injectability.

In summary, the comprehensive characterization of material properties in the ISCD system demonstrates its promising potential for long-acting drug delivery.

Release kinetics and degradation of ISCD *in vitro*

We hypothesize that drug release from ISCD is characterized by drug release from (1) initial burst, (2) diffusion, and (3) degradation of polymers. The initial burst release is attributed to the release of drugs that are not trapped or loosely associated within the polymer network during or after polymerization. The subsequent release rate is dictated by drug diffusion through the polymer matrix and finally polymer degradation via hydrolysis.[23, 32] The structural characteristics of the polymer backbone, along with intrinsic properties such as hydrophilicity, are critical factors that strongly influence these proesses for drug release from the polymer network[33, 34]. The dense mesh network of ISCD made of low molecular weight and hydrophobic PCLDMA plays significant role on sustained release of entrapped drugs as well as their burst release.[35, 36] To alter the polymer mesh network and regulate the release rate of drugs (Figure2 A), we explored the different compositions of ISCDs. The density of polymer networks has been shown to be influenced by several parameters, including polymer chain length, crosslinker concentration, and density of crosslinking groups[37-39]. In addition, the incorporation of hydrophilic polymers has been exploited to increase the water permeability of implants, thereby facilitating drug diffusion throughout the polymer network as well as polymer degradation by erosion and hydrolysis, thereby accelerating the drug release rate[40-42]. Therefore we strategized that conditions leading to a higher drug release from ISCD would include: 1) higher molecular weight PCLDMA, 2) lower concentrations of BPO and DMT, 3) the addition of non-crosslinkable polymers as spacers, and 4) more hydrophilic polymers.

bioRxiv preprint doi: https://doi.org/10.1101/2023.11.04.565631; this version posted November 5, 2023. The copyright holder for this preprint (which was not certified by peer review) is the author/funder, who has granted bioRxiv a license to display the preprint in perpetuity. It is made available under aCC-BY 4.0 International license.

We compared the TAF release from ISCDs made of PCLDMA with two different molecular weights, 630 and 2100 Da, while the rest of the conditions remained the same (Figure S3B). The release profile showed that the depot with the higher molecular weight polymer exhibits higher burst release and faster release kinetics, which indicates that the loose mesh network from longer polymer chain reulsts in the higher release rate from ISCDs. The release profile from ISCDs with varying concentrations of BPO/DMT from 0.1 to 0.4 wt % demonstrated that higher concentrations of the polymerizing agents reduce the drug release showing lower burst releases and slower release rates which we attributed to the reduced polymer mesh size (Figure S3C). Having polymer chains not contributing to crosslinking interfere with the polymerization and lower the crosslinking density.[37] To investigate the impact of incorporating non-crosslinking polymers into ISCD polymer networks and their drug release behaviors, we added 25 wt % non-crosslinkable hydrophilic polymer polyethylene glycol (PEG, MW 400), PCL-diol (MW 530). PEG's oxygen-rich polymer chain promotes strong interactions with water, making it highly hydrophilic[43]. We compared the drug release profile from these ISCDs with three non-crosslinkable polymers with different hydrophilicites and their micro-structure using a scanning electron microscope (SEM) as compared to the control. We found that ISCDs with PEG and PCL-diol, exhibited a significant increase in drug release, reaching 46.5 ± 4.5% ($P < 0.0001$) cumulative release by day 42 post-incubation (Figure 2B). This represents almost twice and 1.5 times the release compared to the control, which achieved 24.5 ± 2.3% release on day 42 post-incubation. These drug release behaviors were consistent with the qualitative assessment using SEM images of the depot morphology (Figure 2F). The ISCDs with PEG, the most hydrophilic polymer among the three spacers, exhibited highly interconnected porous structures, indicating that the uncrosslinked PEG polymer was eroded along with the encapsulated drugs, resulting in enlarged polymer mesh network and thus faster drug release. The ISCDs with PCL-diol also showed signs of erosion with higher roughness on the structure, explaining the greater drug release compared to the pristine PCLDMA ISCDs. ISCDs with PDMS showed low erosion and a smooth cross-section, consistent with their minimal difference in drug release compared to control ISCDs made with PCLDMA. This is attributed to the fact that the strong hydrophobic nature of PDMS prevents its release, making it ineffective as a spacer.[44, 45] Based on these data, we concluded that non-crosslinkable polymers, which can serve as spacers by reducing the crosslink density of the polymer networks, increase the

bioRxiv preprint doi: https://doi.org/10.1101/2023.11.04.565631; this version posted November 5, 2023. The copyright holder for this preprint (which was not certified by peer review) is the author/funder, who has granted bioRxiv a license to display the preprint in perpetuity. It is made available under aCC-BY 4.0 International license.

release profile, especially when their water solubility is higher, by increasing the dissolution of the polymer networks.

We further investigated these ISCDs to confirm the impact of incorporating the polymers with different densities of crosslinking groups on ISCD mesh network by comparing their SEM images and degradation rates to the control ISCDs with pure PCLDMA (Figure 2F). Their degradation data showed that the ISCDs with PEG exhibited a significant increase in degradation rates by month 7, reaching 28.9 ± 2.0 % ($P < 0.0001$), which are almost twice higher than the degradation of control ISCDs. These data supports our hypothesis that the less crosslinked ISCDs would exhibit higher drug release rate due to the enlarged mesh size and the incorporation of polymers with hydrophilic nature, either with or without crosslinking moieties, to the drug delivery systems can be effective way to increase the release profiles.[46, 47]

In vivo pharmacokinetics and biodegradation of ISCD

To assess the pharmacokinetics (PK) of ISCD systems in vivo, 500 µL of 90 mg/mL TAF loaded ISCDs were injected in Sprague Dawley rats (n=3) and compared to the conventional ISFI systems, composed of PLGA 40 wt % dissolved in 55 wt % almond oil, 5 wt % palm oil. Based on in vitro TAF release kinetics study, two ISCD compositions were selected, pristine PCLDMA and PCLDMA with 25 wt % PEGMMA. Plasma samples were collected at hour 4, day 1, 2, 4, 7, 10, week 2, 3, 5, 6, 9, and then at three-week intervals post-injection through month 7. The maximum plasma drug concentration (C_{max}) at 4 hours after subcutaneous injection was 5 and 4 times lower for PCLDMA (133.7 ± 12.7 ng/mL) and PCLDMA/PEGMMA (146.7 ± 27.3 ng/mL) ISCDs, respectively, compared to the ISFI system (668.0 ± 246.0 ng/mL). We attributed the significantly reduced burst release in ISCD platforms compared to ISFI systems to the completely solvent-free formulation of ISCDs. We believe that the high burst release observed in ISFI-injected rats was associated with the solvent efflux and the subsequent water influx during the solidification process of the PLGA component. After the minimal burst release, plasma TAF levels of rats injected with ISCDs containing pure PCLDMA reached less than 10 ng/mL within 10 days and established the sustained level of 1-10 ng/mL up to 200 days. On the other hand, for rats injected with PCLDMA/PEGMMA ISCDs, plasma TAF levels approached below 20 ng/mL by day 10 post-injection, remained 10-20 ng/mL until week 9 post-injeciton, and subsequently exhibited an exponential decrease, reaching levels below the detection limit of 1 ng/mL within 3 months after injection. These ISCD PK data are consistent with in

bioRxiv preprint doi: https://doi.org/10.1101/2023.11.04.565631; this version posted November 5, 2023. The copyright holder for this preprint (which was not certified by peer review) is the author/funder, who has granted bioRxiv a license to display the preprint in perpetuity. It is made available under aCC-BY 4.0 International license.

vitro results indicating that the incorporation of PEGMMA, which is more hydrophilic and less crosslinkable than PCLDMA, into PCLDMA ISCDs results in a higher release profile due to the higher water permeability and looser polymer network. Both compositions of ISCDs showed longer sustained release than ISFI, which showed the high burst release followed by an exponential decline in plasma TAF levels to below the detection limit of 1 ng/mL within 2 months of injection. These results suggest ultra-slow release can be achieved in ISCDs using more than one type of polymer architecture.

We assessed the remaining drug content in the ISCDs 7 months after injection in vivo, and their physiological stability. TAF is known to be unstable in water and could readily degrade in a long-term depot if not adequately protected from the surrounding aqueous environment when stored. At month 7 post injection, the rats were euthanized to retrieve the ISCD implants and the remaining TAF loads were quantified by CHN analysis. Additionally, we dissolved the explanted depots and analyzed the remaining drug using HPLC to find that the reamining drug eluted at the same time as pristine TAF, which confirms that the drug was not degraded during the depot formulation or storage process (Figure S4A) . The TAF dose remaining in the ISCDs was 40.7 ± 8.4% for PCLDMA/ISCDs and 9.1 ± 1.8% for PCLDMA/PEGMMA (Figure 2J), protecting remaining drug from degradation in a solid, whereas almost no drug remained in the ISFI explants (0.26 ± 0.20%) collected at month 2 post-injection (Figure S4B). Notably, ISCDs could be extracted from tissue as a single, easily removable solid depot (Figure 2I), demonstrating superior retrievability, whereas ISFIs were observed as fragile solids, prone to fracture and difficult to extract from tissue (Figure S4C). We measured the mass of the remaining depots to assess the biodegradation of the ISCDs. The remaining mass of ISCDs was 67.1 ± 2.8% for PCLDMA/ISCDs and 45.2 ± 12.1% for PCLDMA/PEGMMA (Figure 2K), indicating that addition of PEGMMA increased the degradation of ISCDs, as expected based on in vitro degradation studies.

In addition, we used magnetic resonance imaging (MRI) to evaluate the long-term morphological changes of ISCDs in vivo and to study the interactions between subcutaneous implants and host tissues at day 1, month 1, and month 7 after injection (Figure 2L). We confirmed that both PCLDMA and PCLDMA/PEGMMA ISCDs did not migrate to other sites or cause adverse tissue reactions. The size of the depots decreased over time, indicating biodegradation, but both depots maintained good structural integrity. Interestingly, at month 7 post injection, we found that the ISCDs incorporated with PEGMMA appeared white on MRI images (marked by the

bioRxiv preprint doi: https://doi.org/10.1101/2023.11.04.565631; this version posted November 5, 2023. The copyright holder for this preprint (which was not certified by peer review) is the author/funder, who has granted bioRxiv a license to display the preprint in perpetuity. It is made available under aCC-BY 4.0 International license.

yellow line for visualization purpose), as did the tissue surrounding the depot, indicating that they had a higher water content than before, while the PCLDMA-only depots remained black. We hypothesize that because PEGMMA is hydrophilic, water may have penetrated the implants as the polymer network loosened over time.

The in vivo pharmacokinetic (PK), biodegradation and MRI studies consistently support the ISCD as a novel biodegradable ultra-long-acting drug delivery system, demonstrating sustained hydrophilic drug delivery over a 7-month period. In particular, the incorporation of a hydrophilic polymer that has a lower cross-linking density than PCLDMA as such, PEGMMA, plays a critical role in modulating the properties of the polymer network, with a pronounced effect on degradation and drug release dynamics in an in vivo context. We believe that the PCLDMA/PEGMMA ISCDs provide an option that can achieve higher systemic levels of therapeutics compared to pure PCLDMA ISCDs by compromising the duration of delivery.

Biocompatibility and retrievability of ISCDs *in vitro*

In vivo biocompatibility is crucial for long-acting injectables to ensure their safe and effective use in patients by minimizing adverse reactions and inflammation.[6, 48] To evaluate the in vivo biocompatibility of the ISCDs, 500 µL of drug-free PCLDMA ISCDs were injected subcutaneously into rats. Samples were explanted at week 1 and month 7 for histological examination. Hematoxylin and eosin (H&E) staining of the specimens revealed the presence of a fibrous capsule around the explanted specimens at week 1, which had disappeared by month 1, indicating a minimal inflammatory response after implantation (Figure 3A,B). In addition, immunohistochemical (IHC) staining for T lymphocytes (CD3) and macrophages (CD68) was performed on the cryosectioned specimens and analyzed both qualitatively and quantitatively to assess the biocompatibility of the constructs (Figure 3B,C). The results showed an initial infiltration of CD3 and CD68 antigens at week 1, likely due to the natural foreign body response. However, this response was significantly reduced by month 1, indicating a high level of biocompatibility for the ISCDs.

Another critical aspect of long-acting injectables is their retrievability.[6, 22] The ability to terminate drug delivery by removing the implant is essential for addressing potential complications or side effects during treatment, allowing for prompt intervention if necessary and ensuring patient well-being throughout the treatment process. To evaluate the retrievability of ISCDs and their ability to efficiently halt drug delivery, we subcutaneously administered TAF-ISCDs to rats (n=3) and removed the implants two weeks later through a small incision near

bioRxiv preprint doi: https://doi.org/10.1101/2023.11.04.565631; this version posted November 5, 2023. The copyright holder for this preprint (which was not certified by peer review) is the author/funder, who has granted bioRxiv a license to display the preprint in perpetuity. It is made available under aCC-BY 4.0 International license.

the injection site on the skin (Fig. 3D, E). We then monitored plasma TAF concentrations at specific intervals: 1, 3, 7, 10, 14, and 21 days post-removal. Upon depot removal, plasma TAF concentrations exhibited an exponential decline, with a more than fourfold decrease within a day to 8.70 ± 5.67 ng/ml and a fourteenfold decrease within a week to 2.99 ± 3.04 ng/mL from the pre-removal plasma level of 43.15 ± 42.80 ng/ml. By day 10 post-retrieval, TAF plasma concentrations had dropped below the limit of detection (1 ng/ml) for two of the rats, with one rat still exhibiting a TAF concentration of 5.7 ng/ml. However, even this rat showed TAF plasma levels below the limit of detection by day 14, indicating that sustained drug release from the ISCD can be effectively halted by implant removal. This retrievability feature enhances the flexibility and safety of our long-acting drug delivery systems.

Compatibility of ISCD with a wide range of therapeutics and combination therapy options

To characterize the release profile of drugs with different physicochemical properties from ISCDs and demonstrate the versatility of our drug delivery systems,[49, 50] we evaluated the in vitro drug release behavior of PCLDMA ISCDs with 8 different small molecule drugs of different hydrophilicity, that includes antiretrovirals, an opiate antagonist, antibiotics, and an immunosuppressant, over 150-360 days, including emtricitabine (FTC), naltrexone (NAL), abacavir (ABC), lamivudine (LAM), vancomycin (VAN), amoxicillin (AMX), and tacrolimus (TAC) in addition to TAF (Figure 4A, Table 1). In general, we observed that hydrophilic drugs with higher water solubility exhibited high initial burst and release rates. Plotting the cumulative release on day 1 for these different therapeutics against their respective water solubility levels revealed a significant positive linear relationship (R^2= 0.7823) (Figure 4B, Table 1), indicating that burst release from the ISCD platform increases with the water solubility of the encapsulated therapeutics. We attribute these results to the higher affinity of hydrophobic drugs for the hydrophobic polymer backbone of PCLDMA[23, 43, 46]. In addition, it is known that hydrophilic drugs can enhance water diffusion into the matrix, thereby accelerating both drug release and polymer erosion and hydrolysis, while hydrophobic drugs tend to inhibit water diffusion into the matrix, slowing down the release rate and polymer degradation[51].

We demonstrated the ability of ISCDs to encapsulate and deliver a combination of two commercial HIV-targeting therapeutics, Epzicom (600 mg ABC and 300 mg LAM) and Descovy (200 mg FTC and 25 mg TAF), by creating two ISCD formulations. One contained 60 mg/mL of ABC and 30 mg/mL of LAM, while the other contained 80

bioRxiv preprint doi: https://doi.org/10.1101/2023.11.04.565631; this version posted November 5, 2023. The copyright holder for this preprint (which was not certified by peer review) is the author/funder, who has granted bioRxiv a license to display the preprint in perpetuity. It is made available under aCC-BY 4.0 International license.

mg/mL of FTC and 10 mg/mL of TAF. We compared the release behavior of these ISCDs when encapsulating single drugs versus the combination of two drugs (Figure 4C,D). In both cases, the ISCDs maintained drug release patterns similar to those of the individual drugs, demonstrating the ability to co-formulate multiple drugs into a single ISCD composition.

To investigate the influence of drug physicochemical properties on pharmacokinetics (PK) and highlight the extended delivery of diverse drugs, we conducted an in vivo PK study utilizing ISCDs loaded with TAC, characterized by higher hydrophobicity than TAF, and NAL, which displays greater hydrophilicity than TAF. Both ISCD formulations consisted of pure PCLDMA and encapsulated 30 mg/mL of TAC and 90 mg/mL of NAL, respectively. These formulations were subcutaneously administered to male Sprague-Dawley rats (n=3), with 500 µL injected per rat. Blood samples were collected at various time points, including hour 4, day 1, 2, 4, 7, 10, week 2, 3, 4, 6, 8, 10, and then at three-week intervals up to month 6 post-injection. We analyzed whole-blood TAC concentrations and plasma NAL concentrations (Figure 4E, F). For both ISCD compositions, drug release exhibited zero-order kinetics after an initial rapid decline in whole blood or plasma concentrations. Upon achieving sustained levels, the rats injected with ISCDs containing NAL, which possesses higher water solubility than TAF, consistently maintained higher plasma NAL concentrations (5-15 ng/mL) compared to the sustained plasma TAF levels in rats with TAF-loaded ISCDs (1-10 ng/mL). In contrast, rats injected with ISCDs containing TAC, a highly hydrophobic molecule, consistently exhibited low whole blood TAC concentrations (0.5-1.5 ng/mL). This variation in release profiles aligns with our in vitro drug release data, confirming that ISCDs containing more hydrophilic therapeutics exhibited higher drug release, both in vitro and in vivo.

Discussion

The development of long-acting drug delivery systems is of immense importance in the field of healthcare, particularly in the context of chronic diseases where consistent medication adherence is critical for therapeutic efficacy.[6, 7, 9, 12, 28, 52, 53] The ISCD presented in this study represents a significant advancement in addressing critical challenges associated with existing drug delivery platforms.

One of the notable achievements of the ISCD platform is its ability to provide sustained release of both hydrophilic drugs, such as TAF and NAL, and hydrophobic drugs, such as TAC, for 180-200 days in vivo. This prolonged delivery time for hydrophilic drugs has not been demonstrated previously.

bioRxiv preprint doi: https://doi.org/10.1101/2023.11.04.565631; this version posted November 5, 2023. The copyright holder for this preprint (which was not certified by peer review) is the author/funder, who has granted bioRxiv a license to display the preprint in perpetuity. It is made available under aCC-BY 4.0 International license.

To achieve this remarkable feat, we utilized a solvent-free formulation that consisted of a hydrophobic, low molecular weight polymer called PCLDMA (MW 630). By employing BPO/DMT polymerizing agents, we were able to create a dense polymer mesh network with PCLDMA, which proved highly effective in efficiently entrapping drugs. This strategic approach minimized burst release and, in turn, enabled the sustained delivery of a wide variety of therapeutic agents. We investigated the intricate factors governing the controlled release kinetics of ISCDs, as evidenced by both in vitro and in vivo experiments. These factors encompassed alterations in the polymer mesh network, including variations in the length and hydrophilic nature of the polymer chain, concentrations of crosslinkers, and the density of crosslinking groups. We elucidated strategies to increase release rates by employing higher molecular weight PCLDMA, lower concentrations of BPO and DMT, the incorporation of non-crosslinkable polymers as spacers, and the utilization of more hydrophilic polymers. Under these conditions, we observed the formation of looser or more hydrophilic polymer networks, making them susceptible to water permeation and depot degradation by erosion or hydrolysis, resulting in higher drug release. Consequently, we harnessed these insights to develop ISCDs incorporating non- or singly-methacrylated PEG into PCLDMA-based formulations, thereby introducing an alternative ISCD platform capable of achieving higher systemic levels of therapeutics compared to pure PCLDMA ISCDs.

The simple formulation and injection process of ISCD renders it particularly appealing in comparison to other ultra-long-acting systems, often burdened by a series of intricate fabrication steps that might restrict widespread adoption. We conducted a comprehensive evaluation of crucial aspects of long-acting injectables, including biocompatibility and retrievability, to ensure the adaptability and safety of the ISCD platform. We have demonstrated successful in vitro delivery of eight different small molecule drugs, each with a different hydrophilicity, for extended periods of time ranging from 150 to 360 days using ISCD, establishing ISCD as a versatile ultra-long-acting delivery platform. Furthermore, our results highlight the importance of considering the physicochemical properties of drugs when formulating ISCDs, with more hydrophilic drugs exhibiting higher release rates. Furthermore, we successfully achieved combined drug delivery using a single ISCD, aligning with the delivery patterns observed in commercial HIV-targeting therapeutics. This adaptability holds significant relevance in the context of combination therapy, a treatment approach that is increasingly prevalent in addressing a variety of diseases.

bioRxiv preprint doi: https://doi.org/10.1101/2023.11.04.565631; this version posted November 5, 2023. The copyright holder for this preprint (which was not certified by peer review) is the author/funder, who has granted bioRxiv a license to display the preprint in perpetuity. It is made available under aCC-BY 4.0 International license.

Taken together, the ISCD represents a groundbreaking paradigm shift in long-acting drug delivery, offering the remarkable capability of sustained release of both hydrophilic and hydrophobic drugs over unprecedented durations. This study provides critical insights into the optimization of drug release kinetics and highlights the ISCD's biocompatibility, retrievability, and ability to deliver multiple drugs simultaneously. This novel platform promises to revolutionize healthcare by addressing the challenges of chronic diseases where consistent medication adherence is critical to therapeutic efficacy.

Methods

Synthesis of methacrylated polycaprolactone (PCL)

20 ml of 530 Da PCL-diol (Sigma-Aldrich) was mixed with 200 ml dichloromethane in a sealed nitrogen-filled flask chilled to 0°C. 33.8 mL of TEA (Sigma-Aldrich) was added to the flask via syringe under stirring at 400 rpm, and 36 mL MAA (Sigma-Aldrich) was subsequently added dropwise via syringe to have three molar eqivalent of TEA and MAA per mol of hydroxy group from PCL-diol. The reaction proceeded for 15 hours under stirring at 0°C. The reaction solvent was removed under reduced pressure and reconstituted in 200 mL of ethyl acetate. This product was washed three times each with saturated aqueous sodium bicarbonate, 0.1 N hydrochloric acid (HCl), and aqueous brine. Following the washing steps, the product was dried with anhydrous sodium sulfate, filtered under vacuum, and solvent was removed under reduced pressure. The crude product was run through a premanufactured silica column (Teledyne Isco) using five column volumes of a mixture of 90% heptane/ 10% ethyl acetate, followed by five column volumes of pure ethyl acetate. Solvent was removed from the latter five fractions under reduced pressure to yield the purified product, PCLDMA, as a viscous yellow liquid. Substitution and purity was confirmed by ^{1}H NMR.

Mechanical characterization

ISCD depots were prepared in cylindrical PDMS molds (6.8 mm diameter, 2.8mm height) for compression test. The dimensions of the depots were then measured using a caliper. The ISCD depots were mounted between plates of a mechanical tester (ADMET) and compressive force was applied to the samples at a rate of 1 mm/min. The compressive strain and stress on the samples were measured and the compressive moduli were obtained from the linear region (0.15-0.25 mm/mm strain) in the stress-strain curve. (n = 4)

Rheological characterization

bioRxiv preprint doi: https://doi.org/10.1101/2023.11.04.565631; this version posted November 5, 2023. The copyright holder for this preprint (which was not certified by peer review) is the author/funder, who has granted bioRxiv a license to display the preprint in perpetuity. It is made available under aCC-BY 4.0 International license.

A rheometer (Discovery HR-3, TA Instruments) equipped with a parallel plate with a gap size of 1 mm and a diameter of 20 mm was used to characterize rheological properties of ISCD pre-polymer solutions. The solutions were prepared as outlined before but without adding polymerization agents, and pipetted onto the rheometer. Any excess solution was trimmed with a spatula before these measurements. The viscosity of the solution was measured while shear rate was swept from 2 to 3700 s^{-1}.

The force required to inject 1 mL of ISCD solution in 30 seconds was measured indirectly from the viscosities using . Briefly, dynamic viscosities, μ, of ISCD solutions were measured and put into the equation below, where L is length of needle (15 mm); Q is volumetric flow rate (2 mL/min); D is inner diameter of syringe barrel (8.66 mm); and d is inner diameter of needle (0.337 mm).

$$F = \frac{32\mu LQD^2}{d^4}$$

Preparation of ISCD for *in vitro* and *in vivo* samples

Pre-polymer solution, composed of methacrylated PCL with or without additives (i.e. PEG, PEGMMA, PEGDMA, PCL, and PDMS), was mixed with 0.1-0.5 wt % of polymerization initiator, BPO. Drugs were incorporated into the polymer blend, followed by 15 seconds of ultrasonication to facilitate a homogeneous suspension. The polymerization accelerator, DMT, was added in at a conetration of 0.1-0.5 wt % and thoroughly mixed, only after all other components had been added. The formulation is drawn into a syringe and injected either into a sink for *in vitro* studies or subcutaneously into a rat for *in vivo* studies. The formulation underwent polymerization into a solid depot within 3-10 minutes after the addition of the accelerator.

In vitro drug analysis

While TAC- and AMX-loaded ISCDs were incubated with 20% methanol in PBS solution due to low water solubility, other ISCD formulations encapsulating different therapeutics were incubated with PBS in a shaker incubator at 37°C. To maintain sink conditions and prevent bacterial growth, the release medium was completely removed and replaced with fresh release medium every week. The release medium was collected at predetermined time points to be analyzed directly or after lyophilization and reconstitution with an appropriate solvent for analysis.

The in vitro cumulative release of TAF was analyzed using NMR. TAF release samples were stored in a -80°C freezer and lyophilized after completely frozen. The remaining powder was reconstituted with 500 μL 0.1 mg/mL

bioRxiv preprint doi: https://doi.org/10.1101/2023.11.04.565631; this version posted November 5, 2023. The copyright holder for this preprint (which was not certified by peer review) is the author/funder, who has granted bioRxiv a license to display the preprint in perpetuity. It is made available under aCC-BY 4.0 International license.

maleic acid in deuterium oxide (D_2O), as an internal standard, and loaded into NMR tubes (NORELL). NMR experiments were performed on an Agilent MR 400 MHz automated NMR system equipped with a 5mm AutoX One probe at room temperature. 64 scans were conducted for each 1H NMR spectrum recording. MestReNova was used for spectrum analysis. Baseline correction of the recorded spectra was performed manually in the software. The maleic acid alkene peak at approximately 6 ppm was integrated, whereas the ppm range of 8.1-8.3 (adenine protons) was integrated and normalized to the maleic acid peak integration area. A 3-point calibration curve was made in a range of 75-300 µg/mL of TAF in D_2O with 0.1 mg/mL maleic acid. The concentration was plotted against the normalized area of integration. The linear regression was generated in Excel and used for all TAF sample quantification.

The in vitro cumulative release of therapeutics, except TAF, in this study was determined by HPLC (Agilent 1260 Infinity II) and the cumulative drug release was calculated. Sample analyses were performed on a ZORBAX 300SB-C18 column (Agilent, 3.0 x 150 mm, 3.5 µm) at 30°C, and all experiments were performed in triplicate. Samples were injected into the HPLC and chromatographic separation was achieved by gradient elution using different mobile phases and flow rates depending on the therapeutics, as described in Table S1-3.

Scanning electron microscopy (SEM) analysis

Surface and microstructures of ISCD were evaluated by SEM. First, polymer solutions were prepared and polymerized in a PBS sink as described above. At predetermined time points, the implants were removed from the sink and dried under low pressure overnight. The lyophilized samples were subsequently mounted on an aluminum stub using carbon tape, and sputter coated with 6 nm of platinum (Leica EM ACE600). The coated samples were then imaged with Hitachi S-4700 FE-SEM.

In vivo pharmacokinetic studies

Male Sprague-Dawley rats (6-8 weeks, Charles River Laboratories) were housed and handled in pathogen-free animal facilities at Brigham and Women's Hospital (BWH) in accordance with a protocol approved by the Institutional Animal Care and Use Committee (IACUC) at BWH. In vivo pharmacokinetic (PK) studies were conducted with different ISCD formulations, either pure PCLDMA or PCLDMA with 25% PEGMMA, with 0.3% BPO/DMT encapsulating tenfovir alafenamide (TAF), naltrexone (NAL), or tacrolimus (TAC). After mixing all ingredients, the ISCD drug formulations were administered subcutaneously with an 18 G needle over the

bioRxiv preprint doi: https://doi.org/10.1101/2023.11.04.565631; this version posted November 5, 2023. The copyright holder for this preprint (which was not certified by peer review) is the author/funder, who has granted bioRxiv a license to display the preprint in perpetuity. It is made available under aCC-BY 4.0 International license.

shoulder of anesthetized rats. At predetermined time points, blood was collected from the tail vein of the rats into EDTA-coated tubes for up to 6-7 months. For analysis of systemic therapeutic levels in rats, whole blood was collected from the tail vein of the rat using a 25-gauge needle and collected in EDTA-coated tubes.

For TAF and NAL samples, the blood sample was centrifuged at 1200g for 10 minutes at 4°C to isolate plasma from the supernatant after centrifugation. The Naltrexone/Nalbuphine Forensic ELISA Kit (Neogen) was used to quantify NAL plasma concentrations according to the manufacturer's instructions. TAF concentrations in plasma samples were analyzed at the PPD Analytical Laboratory (PPD, Inc., Richmond, VA) using reversed-phase high-performance liquid chromatography with UV detection.

To extract TAC from the blood samples, 100 µL of whole blood were combined with 100 µL of MeOH and 50 µL of 0.1M $ZnSO_4$ in an Eppendorf tube, followed by thorough mixing through vortexing. Subsequently, 1 mL of ethyl acetate was added to the mixture and vortexed again. The resulting mixture underwent centrifugation at 14000 rpm for 5 minutes at room temperature. The supernatant was collected and dried, and the measurement of tacrolimus levels was carried out using the Tacrolimus (FK506) ELISA kit (Abbexa, abx515779). The dried TAC sample was reconstituted with the sample diluent buffer provided in the ELISA kit, and further sample analysis was performed following the manufacturer's instructions.

Histological and immunohistochemical analysis

Histological and immunohistochemical analysis were performed on cryosections of the explanted implant samples in order to characterize the inflammatory response elicited by the implanted material. After explantation, samples were fixed in 4% paraformaldehyde for 4 hours, followed by overnight incubation in 30% sucrose at 4 °C. Samples were then embedded in cptimal cutting temperature compound (OCT) and flash frozen in liquid nitrogen. Frozen samples were then sectioned using a Leica Biosystems CM1950 Cryostat. 15-µm cryosections were obtained and mounted in positively charged slides. The slides were then processed for hematoxylin and eosin staining (Sigma) according to instructions from the manufacturer. The stained samples were preserved with DPX mountant medium (Sigma). Immunohistofluorescent staining was performed on mounted cryosections. Anti-CD3 (ab16669) and anti-CD68 (ab125212) (Abcam) were used as primary antibodies, and an Alexa Fluor 594-conjugated secondary antibody (Invitrogen) was used for detection. All sections were counterstained with DAPI (Invitrogen), and visualized on an Leica DMi8 widefield microscope.

bioRxiv preprint doi: https://doi.org/10.1101/2023.11.04.565631; this version posted November 5, 2023. The copyright holder for this preprint (which was not certified by peer review) is the author/funder, who has granted bioRxiv a license to display the preprint in perpetuity. It is made available under aCC-BY 4.0 International license.

Statistical information

All values are presented as mean ± standard deviation. Statistical differences between sample means at each condition were evaluated with two-way ANOVA tests using GraphPad (Software Inc., CA, USA) as P-values were defined as *< 0.05, **< 0.01, ***< 0.001, and ****< 0.0001.

Competing interests

S.L., S.Z, J.M.K. and N.J. have one pending patent based on the ISCD formulation described in this manuscript. J.M.K has been a paid consultant and or equity holder for companies (listed here: https://www.karplab.net/team/jeff-karp) including biotechnologies companies such as Stempeutics, Sanofi, Celltex, LifeVaultBio, Takeda, Ligandal, Camden Partners, Stemgent, Biogen, Pancryos, Element Biosciences, Frequency Therapeutics, Corner Therapeutics, Quthero, and Mesoblast. J.M.K. has been a paid consultant and or equity holder for multiple biotechnology companies. The interests of J.M.K. were reviewed and are subject to a management plan overseen by his institution in accordance with its conflict of interest policies.

References

1. McLellan, A.T., Lewis, D.C., O'brien, C.P. & Kleber, H.D. Drug dependence, a chronic medical illness: implications for treatment, insurance, and outcomes evaluation. *Jama* **284**, 1689-1695 (2000).
2. Sabaté, E. Adherence to long-term therapies: evidence for action. (World Health Organization, 2003).
3. Osterberg, L. & Blaschke, T. Adherence to medication. *New England journal of medicine* **353**, 487-497 (2005).
4. Comer, S.D. et al. Injectable, sustained-release naltrexone for the treatment of opioid dependence: a randomized, placebo-controlled trial. *Archives of general psychiatry* **63**, 210-218 (2006).
5. Swindells, S. et al. Long-acting cabotegravir and rilpivirine for maintenance of HIV-1 suppression. *New England Journal of Medicine* **382**, 1112-1123 (2020).
6. Chaudhary, K., Patel, M.M. & Mehta, P.J. Long-acting injectables: current perspectives and future promise. *Critical Reviews™ in Therapeutic Drug Carrier Systems* **36** (2019).
7. Gigante, A.D., Lafer, B. & Yatham, L.N. Long-acting injectable antipsychotics for the maintenance treatment of bipolar disorder. *CNS drugs* **26**, 403-420 (2012).
8. Heres, S., Kraemer, S., Bergstrom, R.F. & Detke, H.C. Pharmacokinetics of olanzapine long-acting injection: the clinical perspective. *International clinical psychopharmacology* **29**, 299 (2014).
9. Li, L. et al. Long-acting biodegradable implant for sustained delivery of antiretrovirals (ARVs) and hormones. *Journal of Controlled Release* **340**, 188-199 (2021).
10. Pacchiarotti, I. et al. Long-acting injectable antipsychotics (LAIs) for maintenance treatment of bipolar and schizoaffective disorders: A systematic review. *European Neuropsychopharmacology* **29**, 457-470 (2019).
11. Shah, A., Xie, L., Kariburyo, F., Zhang, Q. & Gore, M. Treatment patterns, healthcare resource utilization and costs among schizophrenia patients treated with long-acting injectable versus oral antipsychotics. *Advances in Therapy* **35**, 1994-2014 (2018).
12. Li, W. et al. Clinical translation of long-acting drug delivery formulations. *Nature Reviews Materials* **7**, 406-420 (2022).
13. Nkanga, C.I. et al. Clinically established biodegradable long acting injectables: an industry perspective. *Advanced drug delivery reviews* **167**, 19-46 (2020).

bioRxiv preprint doi: https://doi.org/10.1101/2023.11.04.565631; this version posted November 5, 2023. The copyright holder for this preprint (which was not certified by peer review) is the author/funder, who has granted bioRxiv a license to display the preprint in perpetuity. It is made available under aCC-BY 4.0 International license.

14. Maturavongsadit, P. et al. Biodegradable polymeric solid implants for ultra-long-acting delivery of single or multiple antiretroviral drugs. *International Journal of Pharmaceutics* **605**, 120844 (2021).
15. Stewart, S.A. et al. Development of a biodegradable subcutaneous implant for prolonged drug delivery using 3D printing. *Pharmaceutics* **12**, 105 (2020).
16. Gunawardana, M. et al. Fundamental aspects of long-acting tenofovir alafenamide delivery from subdermal implants for HIV prophylaxis. *Scientific reports* **12**, 8224 (2022).
17. (!!! INVALID CITATION !!! {}).
18. Sitruk-Ware, R. New progestagens for contraceptive use. *Human reproduction update* **12**, 169-178 (2006).
19. Kastellorizios, M., Tipnis, N. & Burgess, D.J. Foreign body reaction to subcutaneous implants. *Immune Responses to Biosurfaces: Mechanisms and Therapeutic Interventions*, 93-108 (2015).
20. Su, J.T. et al. A subcutaneous implant of tenofovir alafenamide fumarate causes local inflammation and tissue necrosis in rabbits and macaques. *Antimicrobial agents and chemotherapy* **64**, 10.1128/aac. 01893-01819 (2020).
21. Goonoo, N. et al. Naltrexone: A review of existing sustained drug delivery systems and emerging nano-based systems. *Journal of Controlled Release* **183**, 154-166 (2014).
22. Benhabbour, S.R. et al. Ultra-long-acting tunable biodegradable and removable controlled release implants for drug delivery. *Nature communications* **10**, 4324 (2019).
23. Joiner, J.B. et al. Effects of drug physicochemical properties on in-situ forming implant polymer degradation and drug release kinetics. *Pharmaceutics* **14**, 1188 (2022).
24. Kempe, S. & Mäder, K. In situ forming implants—an attractive formulation principle for parenteral depot formulations. *Journal of controlled release* **161**, 668-679 (2012).
25. Town, A.R. et al. Tuning HIV drug release from a nanogel-based in situ forming implant by changing nanogel size. *Journal of materials chemistry B* **7**, 373-383 (2019).
26. Bhakay, A., Merwade, M., Bilgili, E. & Dave, R.N. Novel aspects of wet milling for the production of microsuspensions and nanosuspensions of poorly water-soluble drugs. *Drug development and industrial pharmacy* **37**, 963-976 (2011).
27. Loh, Z.H., Samanta, A.K. & Heng, P.W.S. Overview of milling techniques for improving the solubility of poorly water-soluble drugs. *Asian journal of pharmaceutical sciences* **10**, 255-274 (2015).
28. Wright, J.C. & Burgess, D.J. Long acting injections and implants. (Springer, 2012).
29. Mjöberg, B., Pettersson, H., Rosenqvist, R. & Rydholm, A. Bone cement, thermal injury and the radiolucent zone. *Acta Orthopaedica Scandinavica* **55**, 597-600 (1984).
30. Kerin, A., Wisnom, M. & Adams, M. The compressive strength of articular cartilage. *Proceedings of the Institution of Mechanical Engineers, Part H: Journal of Engineering in Medicine* **212**, 273-280 (1998).
31. Watt, R.P., Khatri, H. & Dibble, A.R. Injectability as a function of viscosity and dosing materials for subcutaneous administration. *International Journal of Pharmaceutics* **554**, 376-386 (2019).
32. McHugh, A. The role of polymer membrane formation in sustained release drug delivery systems. *Journal of controlled release* **109**, 211-221 (2005).
33. Correa, S. et al. Translational applications of hydrogels. *Chemical reviews* **121**, 11385-11457 (2021).
34. Li, J. & Mooney, D.J. Designing hydrogels for controlled drug delivery. *Nature Reviews Materials* **1**, 1-17 (2016).
35. Bibby, D.C., Davies, N.M. & Tucker, I.G. Mechanisms by which cyclodextrins modify drug release from polymeric drug delivery systems. *International journal of pharmaceutics* **197**, 1-11 (2000).
36. Commandeur, S., van Beusekom, H.M. & van der Giessen, W.J. Polymers, drug release, and drug‐eluting stents. *Journal of interventional cardiology* **19**, 500-506 (2006).
37. Radi, B., Wellard, R.M. & George, G.A. Effect of dangling chains on the structure and physical properties of a tightly crosslinked poly (ethylene glycol) network. *Soft Matter* **9**, 3262-3271 (2013).
38. Wisniewska, M.A., Seland, J.G. & Wang, W. Determining the scaling of gel mesh size with changing crosslinker concentration using dynamic swelling, rheometry, and PGSE NMR spectroscopy. *Journal of Applied Polymer Science* **135**, 46695 (2018).
39. Rehmann, M.S. et al. Tuning and predicting mesh size and protein release from step growth hydrogels. *Biomacromolecules* **18**, 3131-3142 (2017).
40. Khan, N.A. et al. Preparation and Characterization of Hydrophilic Polymer Based Sustained-Release Matrix Tablets of a High Dose Hydrophobic Drug. *Polymers* **14**, 1985 (2022).

bioRxiv preprint doi: https://doi.org/10.1101/2023.11.04.565631; this version posted November 5, 2023. The copyright holder for this preprint (which was not certified by peer review) is the author/funder, who has granted bioRxiv a license to display the preprint in perpetuity. It is made available under aCC-BY 4.0 International license.

41. Woodard, L.N. & Grunlan, M.A. (ACS Publications, 2018).
42. Lyu, S. & Untereker, D. Degradability of polymers for implantable biomedical devices. *International journal of molecular sciences* **10**, 4033-4065 (2009).
43. Li, K., Qi, Y., Zhou, Y., Sun, X. & Zhang, Z. Microstructure and properties of poly (ethylene glycol)-segmented polyurethane antifouling coatings after immersion in seawater. *Polymers* **13**, 573 (2021).
44. DiFilippo, E.L. & Eganhouse, R.P. Assessment of PDMS-water partition coefficients: implications for passive environmental sampling of hydrophobic organic compounds. *Environmental science & technology* **44**, 6917-6925 (2010).
45. Lee, J.N., Park, C. & Whitesides, G.M. Solvent compatibility of poly (dimethylsiloxane)-based microfluidic devices. *Analytical chemistry* **75**, 6544-6554 (2003).
46. Lee, S., Tong, X. & Yang, F. The effects of varying poly (ethylene glycol) hydrogel crosslinking density and the crosslinking mechanism on protein accumulation in three-dimensional hydrogels. *Acta biomaterialia* **10**, 4167-4174 (2014).
47. Sheridan, G.S. & Evans, C.M. Understanding the roles of mesh size, T g, and segmental dynamics on probe diffusion in dense polymer networks. *Macromolecules* **54**, 11198-11208 (2021).
48. Mi, F.-L., Tan, Y.-C., Liang, H.-F. & Sung, H.-W. In vivo biocompatibility and degradability of a novel injectable-chitosan-based implant. *Biomaterials* **23**, 181-191 (2002).
49. Sax, P.E. et al. Abacavir/lamivudine versus tenofovir DF/emtricitabine as part of combination regimens for initial treatment of HIV: final results. *Journal of Infectious Diseases* **204**, 1191-1201 (2011).
50. Argyo, C., Weiss, V., Bräuchle, C. & Bein, T. Multifunctional mesoporous silica nanoparticles as a universal platform for drug delivery. *Chemistry of materials* **26**, 435-451 (2014).
51. Siegel, S.J. et al. Effect of drug type on the degradation rate of PLGA matrices. *European Journal of Pharmaceutics and Biopharmaceutics* **64**, 287-293 (2006).
52. Bassand, C. et al. Smart design of patient-centric long-acting products: from preclinical to marketed pipeline trends and opportunities. *Expert opinion on drug delivery* **19**, 1265-1283 (2022).
53. Brissos, S., Veguilla, M.R., Taylor, D. & Balanzá-Martinez, V. The role of long-acting injectable antipsychotics in schizophrenia: a critical appraisal. *Therapeutic advances in psychopharmacology* **4**, 198-219 (2014).

bioRxiv preprint doi: https://doi.org/10.1101/2023.11.04.565631; this version posted November 5, 2023. The copyright holder for this preprint (which was not certified by peer review) is the author/funder, who has granted bioRxiv a license to display the preprint in perpetuity. It is made available under aCC-BY 4.0 International license.

Figures

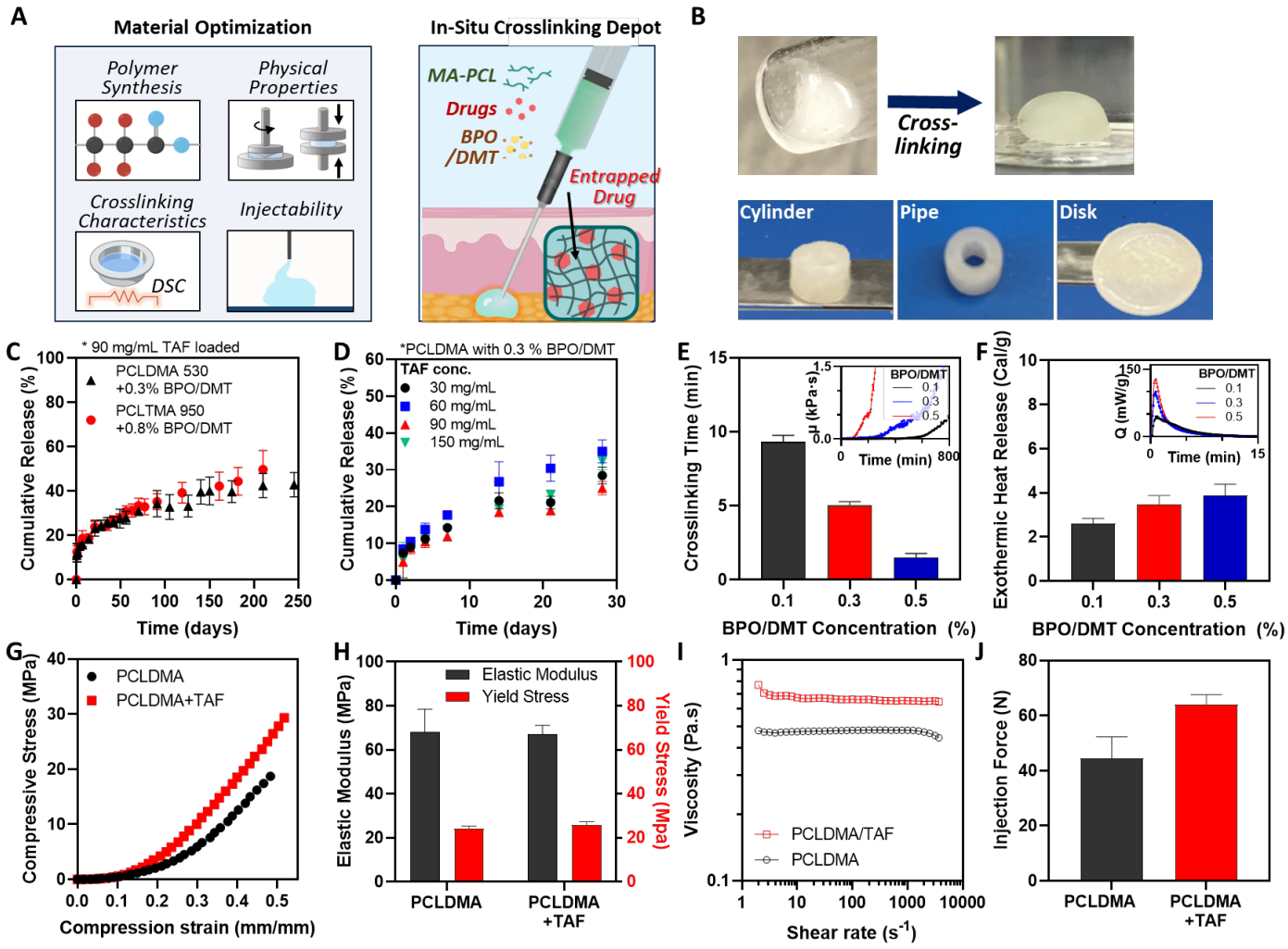

Figure 1. Preparation and material characterization of ISCD (A) A schematic illustration of material optimization process and polymerization of ISCD. (B) The camera images shows the sol-gel transition of ISCD. (C) In vitro release profile of tenofovir alafenamide TAF from ISCDs made of either PCLDMA with 0.8 % of both BPO and DMT or PCLDMA with 0.3 % of both BPO, demonstrating ultra long-acting delivery of the hydrophilic drug. (D) In vitro release profile of TAF from ISCDs with different doses of TAF, showing that the release profiles from ISCDs are similar within the range of 30-150 mg/mL TAF encapsulation. (E) The time required for polymerizing ISCDs with varying concentrations of BPO/DMT, illustrating a reduction in crosslinking time at higher concentrations of the polymerization agents. The inset shows that in measuring the crosslinking time, we monitor the increase in viscosities of ISCDs with different BPO/DMT concentrations. (F) Exothermic heat released during the crosslinking of ISCDs with varying concentrations of BPO/DMT shows that there is no

bioRxiv preprint doi: https://doi.org/10.1101/2023.11.04.565631; this version posted November 5, 2023. The copyright holder for this preprint (which was not certified by peer review) is the author/funder, who has granted bioRxiv a license to display the preprint in perpetuity. It is made available under aCC-BY 4.0 International license.

significant heat generation, thus alleviating concerns of potential thermal tissue damage during the procedure. (G) Compressive stress–strain curves for ISCDs both with and without TAF encapsulated, from which (H) the elastic moduli and yield stress are obtained. (I) Viscosities of pre-polymerized ISCDs both with and without TAF encapsulated, which are used to calculate (J) the injection forces required to inject at 2 mL/min using a 1 mL syringe with a 23G nozzle.

bioRxiv preprint doi: https://doi.org/10.1101/2023.11.04.565631; this version posted November 5, 2023. The copyright holder for this preprint (which was not certified by peer review) is the author/funder, who has granted bioRxiv a license to display the preprint in perpetuity. It is made available under aCC-BY 4.0 International license.

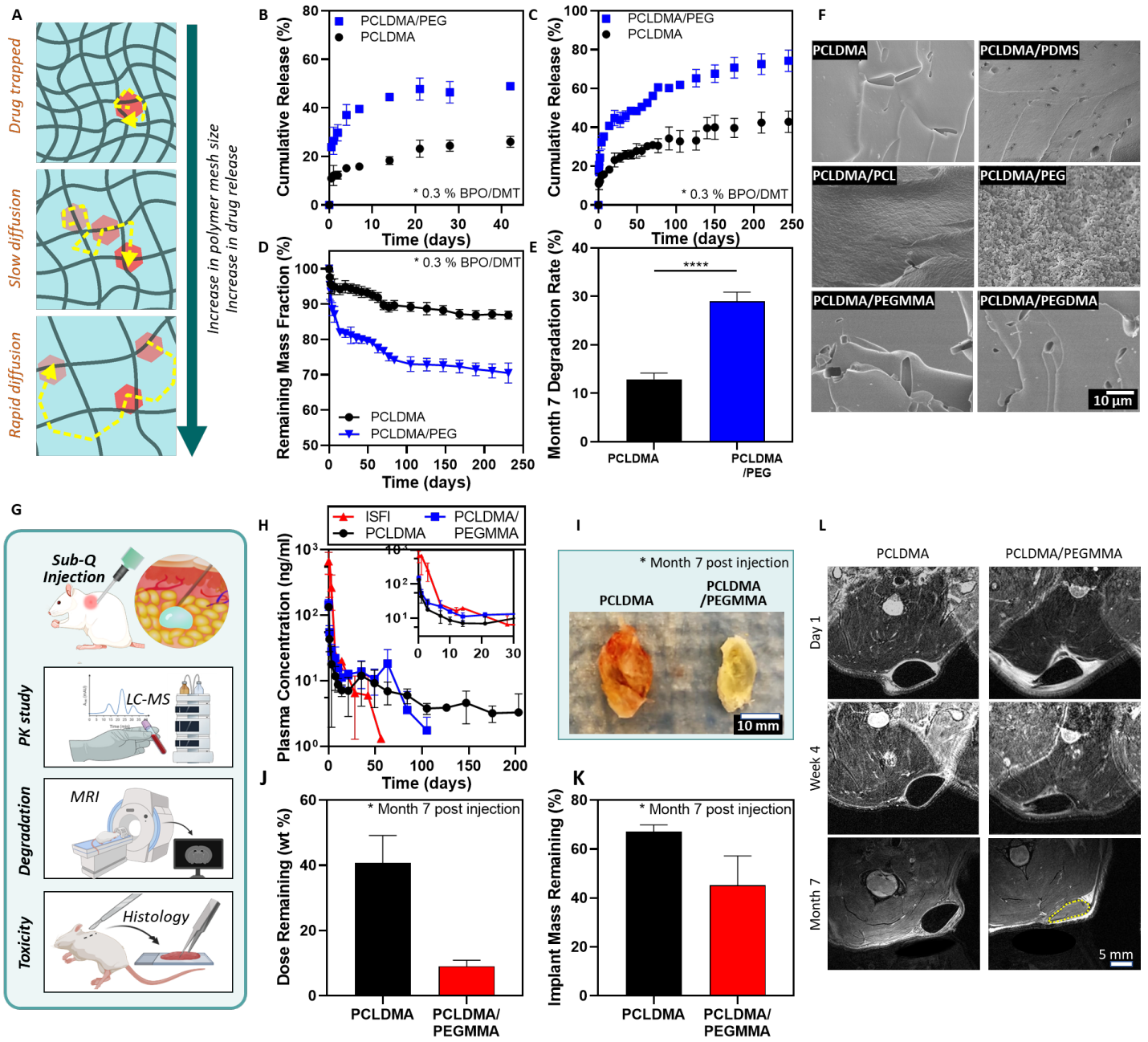

Figure 2. Characterization and control of release kinetics and degradation of ISCDs *in vitro* and *in vivo*

(A) The pharmacokinetics and degradation of ISCD can be tailored by modifying their polymer mesh network. (B) *In vitro* release profiles of TAF from ISCDs made of PCLDMA and PCLDMA with 25% PEG, PCL, and PDMS, demonstrating an increased release with the incorporation of more hydrophilic polymers into ISCDs. (C) *In vitro* release of TAF and (D) degradation behavior of ISCDs composed of PCLDMA and PCLDMA with 25 % of PEG, PEGMMA and PEGDMA, demonstrating reduced release as well as degradation rates as PEGs with higher

bioRxiv preprint doi: https://doi.org/10.1101/2023.11.04.565631; this version posted November 5, 2023. The copyright holder for this preprint (which was not certified by peer review) is the author/funder, who has granted bioRxiv a license to display the preprint in perpetuity. It is made available under aCC-BY 4.0 International license.

degree of crosslinkable groups are introduced. (E) Degradation rate of ISCDs composed of PCLDMA and PCLDMA with 25 % of PEG, PEGMMA and PEGDMA at month 7 post-incubation in vitro. (F) SEM images of ISCDs made of PCLDMA and PCLDMA with different polymer additives to show the cross section of depot structure at week 1 post incubation *in vitro*. (G) ISCD was subcutaneously injected into rats to assess the in vivo pharmacokinetics, biodegradation, and biocompatibility of ISCD. (H) *In vivo* pharmacokinetics of TAF from three different injectable implants, including ISFI as a control and ISCDs made of PCLDMA and PCLDMA with PEGMMA, demonstrating an enhanced release profile of ISCDs when compared to ISFI. (I) Camera images of retrieved ISCDs made of PCLDMA and PCLDMA with PEGMMA at month 7 post-injection and (J) the remaining TAF loads and (K) total mass of them. (L) MRI images of subcutaneously injected ISCDs on rats, to monitor the degradation of ISCDs composed of PCLDMA and PCLDMA with PEGMMA for 7 months.

bioRxiv preprint doi: https://doi.org/10.1101/2023.11.04.565631; this version posted November 5, 2023. The copyright holder for this preprint (which was not certified by peer review) is the author/funder, who has granted bioRxiv a license to display the preprint in perpetuity. It is made available under aCC-BY 4.0 International license.

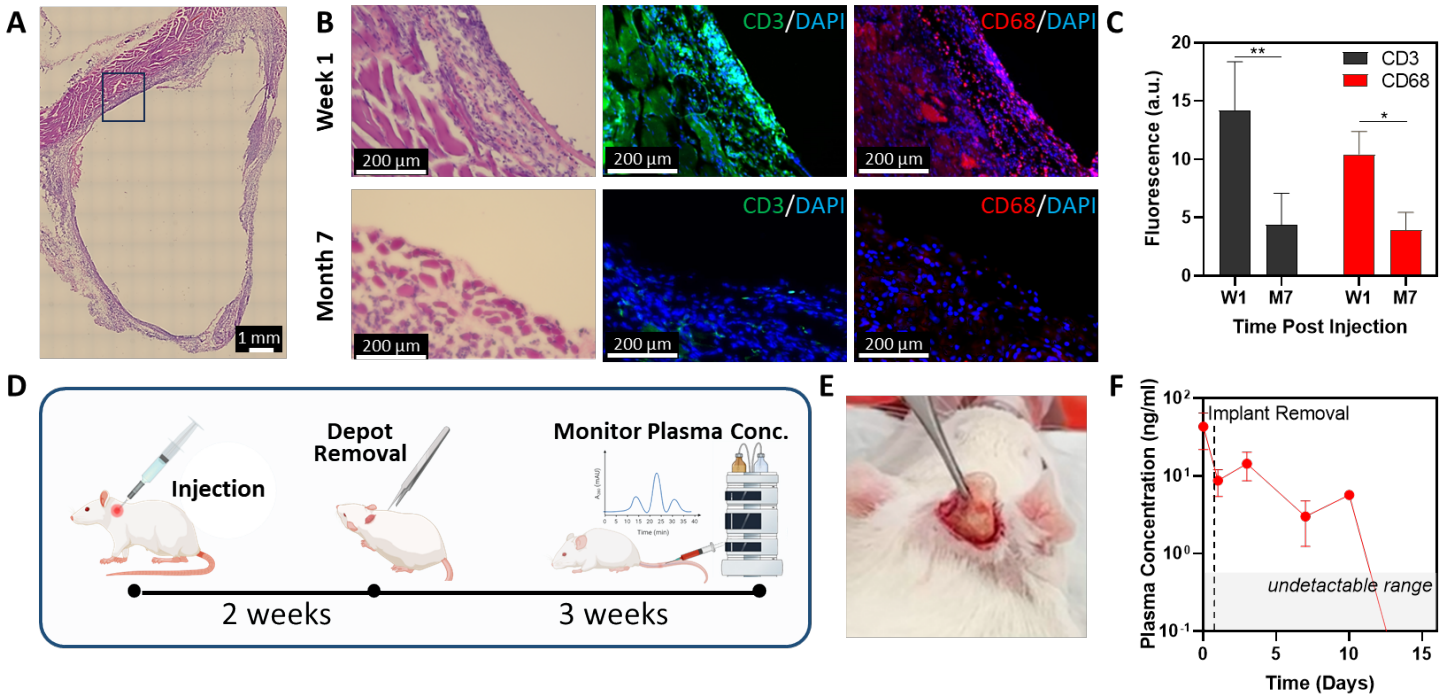

Figure 3. Evaluation of biocompatibility and retrievability of ISCD (A) H&E staining of the ISCD and subcutaneous tissue at week 1. (B) H&E (left) and IHC staining against CD3, (middle, green) and CD68 markers (right, red) showing the interface between implanted depot and tissues at week 1 (top) and month 6 (down) post-injection. (C) Inflammatory response quantified by calculating fluorescence intensity from IHC images. (D) Timeline of ISCD retrieval study to monitor the reduction in plasma concentration of TAF. (E) Camera image taken during the procedure to remove the ISCD from a rat, showing retrievability of ISCD. (F) Plasma concentration of TAF after implant removal

bioRxiv preprint doi: https://doi.org/10.1101/2023.11.04.565631; this version posted November 5, 2023. The copyright holder for this preprint (which was not certified by peer review) is the author/funder, who has granted bioRxiv a license to display the preprint in perpetuity. It is made available under aCC-BY 4.0 International license.

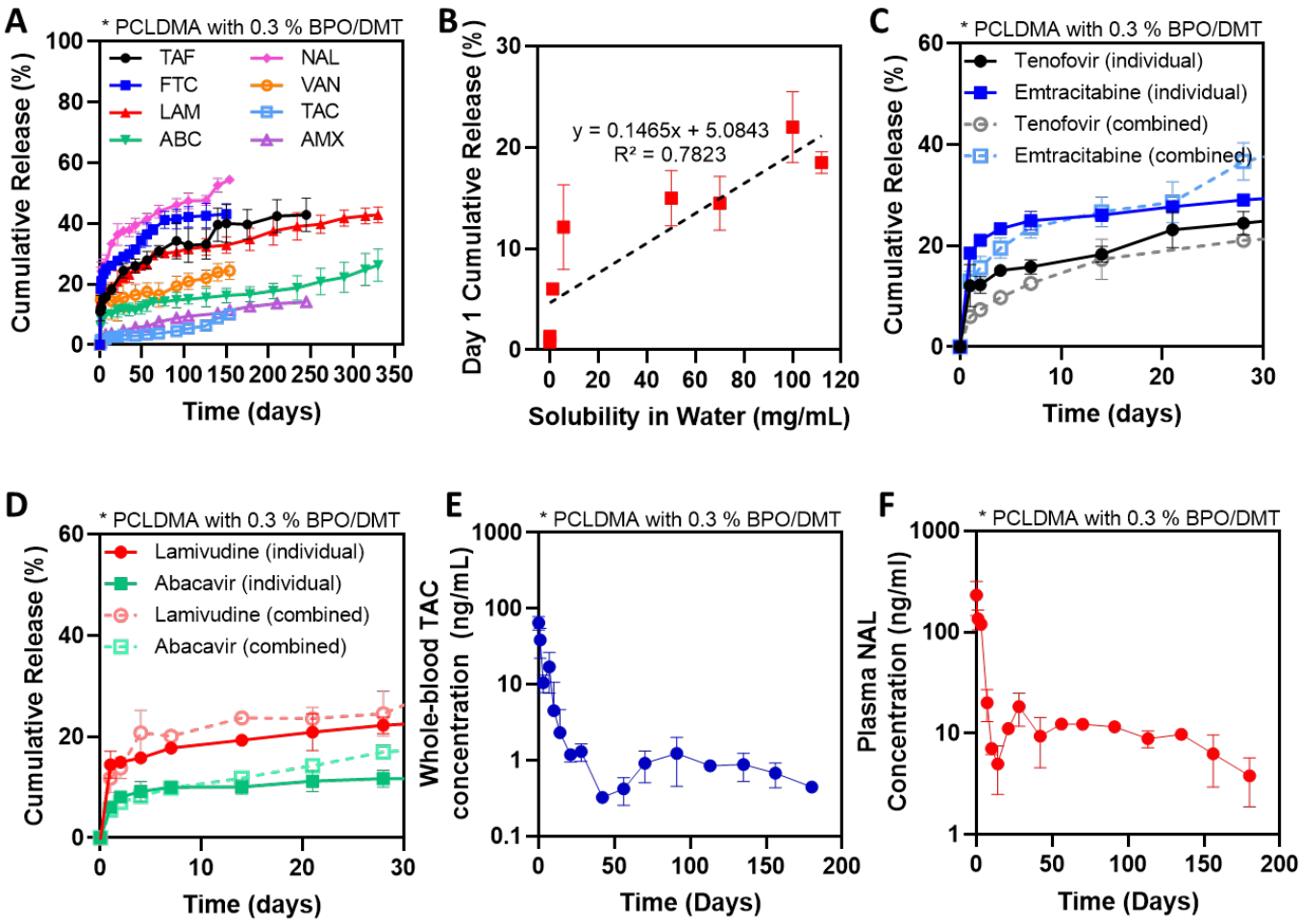

Figure 4. Versatility of ISCD for encapsulating a range of therapeutics with varying levels of hydrophilicity. (A) *In vitro* release profiles of various therapeutics with diverse hydrophilicities. (B) Cumulative release at day 1 post-injection, initial burst release, as a function of the water solubility of therapeutics. (C) In vitro release profile of ISCDs with TAF and FTC, comparing the release when drugs are encapsulated individually and when a combination of two drugs is within a single ISCD. (D) In vitro release profile of ISCDs with ABC and LAM, comparing the release when drugs are encapsulated individually and when a combination of two drugs is within a single ISCD. (E) Whole blood concentration of TAC from subcutaneously injected ISCDs in rats. (F) Plasma concentration of NAL from subcutaneously injected ISCDs in rats.

bioRxiv preprint doi: https://doi.org/10.1101/2023.11.04.565631; this version posted November 5, 2023. The copyright holder for this preprint (which was not certified by peer review) is the author/funder, who has granted bioRxiv a license to display the preprint in perpetuity. It is made available under aCC-BY 4.0 International license.

Tables

Table 1 Initial burst release against water solubility of therapeutics

Drug	Solubility (mg/ml)	Day 1 cumulative release (%)
FTC	112	18.51
NAL	100	22.02
ABC	1.21	6.04
LAM	70	14.5
VAN	50	14.98
TAF	5.63	12.14
AMX	0.011	0.79
TAC	0.004	1.34